A universal dynamical metabolic model representing mixotrophic growth of Chlorella sp. on wastes

Bruno Assis Pessi, Caroline Baroukh, Anais Bacquet, Olivier Bernard

A universal dynamical metabolic model representing mixotrophic growth of *Chlorella* sp. on wastes

Bruno Assis Pessi[a], Caroline Baroukh[b], Anais Bacquet[c], Olivier Bernard[a,c]

[a] *Biocore, INRIA, Université Côte d'Azur, Sophia Antipolis, France*
[b] *LIPME, Université de Toulouse, INRAE, CNRS, Castanet Tolosan, France*
[c] *LOV, UMR 7093, Sorbonne university, CNRS, Villefranche-sur-mer*

Abstract

An emerging idea is to couple wastewater treatment and biofuel production using microalgae to achieve higher productivities and lower costs. This paper proposes a metabolic modelling of *Chlorella sp.* growing on fermentation wastes (blend of acetate, butyrate and other acids) in mixotrophic conditions, accounting also for the possible inhibitory substrates. This model extends previous works by modifying the metabolic network to include the consumption of glycerol and glucose by *Chlorella sp.*, with the goal to test the addition of these substrates in order to overcome butyrate inhibition. The metabolic model was built using the DRUM framework and consists of 188 reactions and 173 metabolites. After a calibration phase, the model was successfully challenged with data from 122 experiments collected from scientific literature in autotrophic, heterotrophic and mixotrophic conditions. The optimal feeding strategy estimated with the model reduces the time to consume the volatile fatty acids from 16 days to 2 days. The high prediction capability of this model opens new routes for enhancing design and operation in waste valorisation using microalgae.

Keywords: Chlorella, metabolic modelling, heterotrophy, mixotrophy, diauxic growth, dynamical modelling

1. Introduction

Microalgae have been extensively studied during the past decade. Some species are capable of producing lipids or carbohydrates that can in turn be converted into biofuel (Sajjadi et al., 2018). Microalgae use light energy, via photosynthesis, to fix carbon dioxide. Not only, their growth rate is much faster than that of higher plants, but they can also be cultivated in wastewater, reducing the environmental impact of bioproducts (Morales et al., 2019, Arashiro et al., 2022). An emerging idea suggests using wastewater treatment to obtain biofuels as a co-product (Barsanti and Gualtieri, 2018). Even though the production efficiency appears to be attractive,

many optimization steps still need to be carried out for this process to become sufficiently cost-effective and environmentally-friendly (Tan et al., 2018).

There is already an extensive list of works about wastewater treatment with microalgae. Nevertheless there is no unified framework for the modeling of this process (Shoener et al., 2019). Most of these models are variants of active sludge models (ASM) and anaerobic digestion models (ADM), which were originally designed for bacterial systems (Casagli et al., 2021b, Wágner et al., 2016). In addition mixotrophy is rarely considered in these models and microalgae are assumed to grow autotrophically, neglecting the simultaneous use of organic compounds. In contrast to these models, metabolic models can acquire the reaction yields, including photosynthesis and organic carbon uptake by using the knowledge of the biochemical reactions taking place in the organism which is reconstructed from genomic data. Despite this, less than 5% of models of water recover facilities have metabolic reconstructions and usually rely on empirical yield coefficients (Shoener et al., 2019). Metabolic models also have the advantage of estimating internal metabolic fluxes, providing valuable information for future strain improvement via metabolic engineering. Nevertheless, the applicability of metabolic models to predict dynamical systems is constrained by the size of the metabolic network - which in genome scale models usually consists of thousands of reactions and metabolites. Consequently, to embed mixotrophic microalgal models in larger frameworks representing the mass fluxes within the wastewater process, it is necessary to use techniques to reduce the metabolic models to a reasonable size, while still keeping the phenotype of the original network.

The development of techniques to reduce the size of metabolic networks started more than 20 years ago (Singh and Lercher, 2020). Since then new methods have been developed relying on a variety of different approaches, such as linear programming, graph-based search and elementary flux modes (Singh and Lercher, 2020). Our increasing understanding of genomic information led to the construction of more complex genome scale networks. This has motivated the field of bioinformatics to research new ways to reduce and analyze metabolic models, consequently new methods are still being developed (Küken et al., 2021, Hameri et al., 2021). The choice of the reduction method will depend on the intentions of the modeler, the wished degree of flexibility of the phenotype prediction and the final size of the model. In this work, we will rely on the DRUM framework (Baroukh et al., 2014, 2016), which although requires input from the modeler and prior knowledge about the network, it is able to reproduce behaviour outside the steady state, while greatly reducing the number of metabolites and reactions in the final model. On top of this, such dynamic model can support a control strategy to enhance process efficiency.

During dark fermentation of organic wastes, anaerobic bacteria and archaea convert complex and non-assimilable compounds into Volatile Fatty Acids (VFAs) us-

able by microalgae. Indeed, VFAs can support heterotrophic growth of microalgae, while they use ammonium and phosphate in the wastewater as source for nitrogen and phosphorus (Baroukh et al., 2017, Turon et al., 2015b,a, Gao et al., 2022). In this perspective, *Chlorella sp.* was selected for its potential in associating biofuel production with effluent treatment (Casagli et al., 2021b, Gao et al., 2022, Wágner et al., 2016). Indeed, this species can accumulate up to 50% of its dry weight in lipids, essentially in the form of triacylglycerol (TAG). In addition, its capacity to grow in the main dark fermentation effluents has been demonstrated, under heterotrophic or mixotrophic conditions (Turon et al., 2015a, Lacroux et al., 2022). The VFA mixture resulting from dark fermentation is typically made of a blend composed of about 30% acetate and 70% butyrate. Other organic acids can also be found (Rafrafi et al., 2013, Turon et al., 2015a), among which lactate, which is not consumed and does not affect the growth of *Chlorella* (Turon et al., 2015a). Turon et al. (2015a) first proposed a kinetic model of the consumption of butyrate and acetate by *Chlorella*. Later, an extended metabolic model was proposed using the DRUM framework (Baroukh et al., 2017). Here, we extend further this model by including the consumption of glucose and glycerol by *Chlorella* and propose a universal multi-substrate dynamic reduced metabolic model.

This model is the cornerstone for tackling the major issue due to the high concentration of butyrate which is slowly consumed by microalgae and inhibited by acetate (Hu et al., 2012, Turon et al., 2015b, Lacroux et al., 2022). To address this problem, another organic substrate can be added to lever the inhibition effect of butyrate and eventually accelerate growth in dark fermentation effluents. Microalgae will first use a more efficient carbon substrate to reach a higher biomass concentration. It follows that acetate will be faster consumed, and in the end butyrate. Glucose could ideally play this role, but its cost is not compatible with process economics. Acetate addition is more reasonable but would generate large variations in pH. Glycerol is a by-product of biodiesel synthesis by transesterification. Its low cost is likely to be compensated by the enhanced microalgal productivity. Developing a mixotrophic multi-substrate metabolic model is the main objective of this paper, and such approach can be used to identify strategies to more efficiently use dark fermentation products and optimize their conversion into algal biomass.

The model developed here represents, in detail, the growth under different autotrophic, heterotrophic and mixotrophic conditions and for four organic substrates. To our knowledge, this is the first model including such a large range of potential substrates in mixotophic regimes. The model was validated in different cultivation conditions using the abundant literature available on autotrophic, heterotrophic or mixotrophic growth of *Chlorella*. To this end, data from 122 experiments was extracted from 15 publications, amounting to more than 2600 concentration data points (see Table 1), thus reaching an unprecedented level of validation. This model

Table 1: Considered experiments for each substrate. In parenthesis, the number of experiments in mixotrophic conditions out of the total experiments.

Substrate	# exp.	Species	References
Glycerol	12 (9)	*C. sorokiniana*	León-Vaz et al. (2019)
		C. sp.	Sen and Martin (2018)
		C. protothecoides	Chen and Walker (2011), O'Grady and Morgan (2011)
		C. vulgaris	Ma et al. (2016)
Glucose	22 (11)	*C. sorokiniana*	León-Vaz et al. (2019), Li et al. (2013, 2014)
		C. protothecoides	Espinosa-Gonzalez et al. (2014), Chen and Walker (2011)
		C. pyrenoidosa	Ogbonna et al. (1997)
Glucose/Glycerol	2 (2)	*C. protothecoides*	O'Grady and Morgan (2011)
Acetate	40 (25)	*C. sorokiniana*	León-Vaz et al. (2019), Turon et al. (2015a,b), Chen et al. (2017a,b), Xie et al. (2020a)
		C. sacchrarophila	Xie et al. (2020b)
Butyrate	10 (4)	*C. sorokiniana*	Turon et al. (2015b,a)
Acetate/Butyrate	23 (6)	*C. sorokiniana*	Turon et al. (2015b,a)
Autotrophic	13	*C. sorokiniana*	Li et al. (2014), León-Vaz et al. (2019), Turon et al. (2015b,a)
		C. sp.	Sen and Martin (2018)

is shown to support a strategy to enhance the bioconversion of VFA into microalgal biomass by managing the way the different substrates are supplied.

2. Materials and methods

2.1. General Principles of the DRUM approach

The dynamic model development follows the DRUM (Dynamic Reduction of Unbalanced Metabolism) approach. The full description and complete explanation of the approach is available in Baroukh et al. (2014).

Briefly, the metabolism of a microorganism can be described by its metabolic network composed of a set of n_r biochemical reactions (here $n_r = 188$) involving

n_m metabolites (here $n_m = 173$) and represented by the stoichiometric matrix $K \in \mathcal{R}^{n_m \times n_r}$ (see Appendix for the full list of reactions and metabolites). The biomass B is produced from a set of substrates S and excretes a set of products P. In a perfectly mixed reactor with a constant volume, the system can be described by the following set of ordinary differential equations:

$$\frac{dM}{dt} = \frac{d}{dt}\begin{pmatrix} S \\ C \\ P \\ B \end{pmatrix} = \begin{pmatrix} K_S \\ K_C \\ K_P \\ K_B \end{pmatrix} .v(M).B - DM + DM_{in} = K.v(M).B - DM + DM_{in} \quad (1)$$

where M represents the vector of the concentrations of metabolites composed of substrate (S), intracellular metabolites (C), excreted products (P) and biomass (B). M_{in} is the influent concentration of these quantities. The dilution rate of the reactor (ratio of influent flow rate over the reactor volume) is D ($D = 0$ for a batch process). All the concentrations are expressed as total concentrations in the solution. $v \in \mathcal{R}^{n_r}$ is the reaction kinetic vector, while the matrices $K_S \in \mathcal{R}^{n_S \times n_r}$, $K_C \in \mathcal{R}^{n_C \times n_r}$, $K_P \in \mathcal{R}^{n_P \times n_r}$ and $K_B \in \mathcal{R}^{1 \times n_r}$ correspond, respectively, to the stoichiometric matrices of substrates S, products P, intracellular metabolites C and biomass B ($n_S + n_C + n_P + 1 = n_m$).

In metabolic models, intracellular metabolites are generally assumed to be quasi-stationary ($\frac{dC}{dt} = K.v = 0$), i.e. they are assumed to be consumed as soon as they have been synthesised. However, in the case of microalgae, this hypothesis has proven to be false for certain of its metabolites (denoted A) during mixotrophic or autotrophic growth (Baroukh et al., 2014, 2017). The DRUM method (Baroukh et al., 2014), consists in dividing the metabolic network into n quasi-stationary subnetworks ($K = (K_{SN_1}, \ldots, K_{SN_n})$, $K_{SN_i}.v_{SN_i} = 0 \; for \; i \in 1, \ldots, n$). These are linked by the A metabolites that are, in contrast, non-stationary, can accumulate and be later consumed. This division into subnetworks is justified by the presence of metabolic pathways that correspond to metabolic functions, to reaction groups that are regulated simultaneously and to the presence of compartments within the cell. Cellular mechanisms are therefore employed for assessing the subnetwork. Hence, the A metabolites can either be found at the junction of several metabolic pathways, or they can be transported from one compartment to another, or they can be final products that accumulate in the cell. The system of ordinary differential equations (1) therefore becomes:

$$\frac{dM'}{dt} = \frac{d}{dt}\begin{pmatrix} S \\ A \\ P \\ B \end{pmatrix} = \begin{pmatrix} K_S \\ K_A \\ K_P \\ K_B \end{pmatrix} .\alpha.B = K'.\alpha.B - DM' + DM'_{in} \quad (2)$$

With K' the stoichiometric matrix of macroscopic reactions obtained through the analysis of elementary modes (Schuster et al., 1999) on the subnetworks, and α the kinetic vector associated to these macroscopic reactions. B now represents the structural biomass, i.e. the fraction of biomass that does not contain the inert compartments of reserve A. The total biomass can be deduced using a mass balance of the elemental compounds (C, N, P, O, ...).

2.2. Construction of the model

The core of the metabolic network from Baroukh et al. (2017) has been used and modified in order to add the glucose and glycerol consumption pathways (Figure 1). This network contains the central autotrophic, mixotrophic and heterotrophic metabolic pathways including photosynthesis, glycolysis, the pentose phosphate pathway, the Krebs cycle, oxidative phosphorylation and the synthesis of chlorophyll, carbohydrates (e.g. starch), amino-acids and nucleotides. The synthesis pathways of macromolecules such as proteins, lipids, starch, DNA, RNA as well as the functional biomass are represented through macroscopic reactions.

The DRUM method requires the partitioning of the metabolism into subnetworks as well as the identification of the metabolites, in between the subnetworks, which can accumulate. The subnetworks are defined by their metabolic function and/or their affiliation to a cellular compartment. Different partitions among the 188 reactions have been tested, with a view to select the one which minimized the number of parameters to assess while providing a correct representation of the experimental data. The best result was obtained when the network is divided into four subnetworks (Figure 1), corresponding to, 1) the glyoxysome, 2) the chloroplast, 3) the absorption of glycerol and 4) the synthesis of biomass. The glyoxysome and chloroplast subnetworks remain unchanged in comparison with the initial Baroukh et al. (2017) model.

The macroscopic reactions associated to each subnetwork are deduced from the elementary mode analysis (Klamt and Stelling, 2003). The Matlab "efmtool" was run to calculate the Elementary Flux Modes (EFMs) (Terzer and Stelling, 2008). In total, $86,142$ EFMs including $3,310$ associated to futile cycles (dissipation of carbon substrate in the form of CO_2) have been achieved. These macroscopic reactions are further used to determine the mass fluxes in the different parts of the network by assembling reactions belonging to the same kinetics.

2.3. Analysis of the sub-networks

2.3.1. Motivations

In this section, we present the macroscopic reactions which result from the reduction of each subnetwork by the computation of the EFMs. As recommended by Baroukh et al. (2014), the reaction kinetics must be mathematically represented

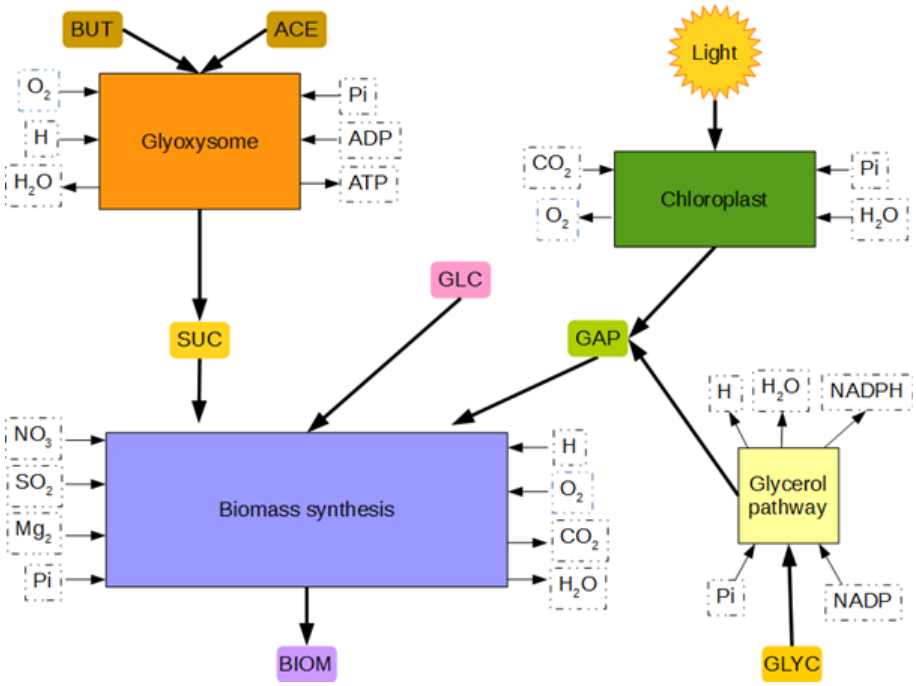

Figure 1: Considered metabolic subnetworks to represent growth of *Chlorella* on a mixture of glycerol, glucose, acetate and butyrate

	Subnetwork	Macroscopic reaction
MR_1	Glyoxysome	2 ACE + 3.5 H + 0.5 $O_2 \rightarrow SUC + 0.5\ H_2O$
MR_2		$BUT + 7H + 1.5O_2 \rightarrow SUC + 5H_2O$
MR_3	Chloroplast	$Light + 3CO_2 + 2H_2O + Pi \rightarrow GAP + 3O_2$
MR_4	Glycerol pathway	$GLY + Pi \rightarrow GAP + H_2O$
$MR_5(NH_4)$	Biomass synthesis	$4.15\ GAP + 2.54O_2 + 0.99NH_4 + 0.02SO_4 + 0.01Mg_2 \rightarrow B + 0.99H + 2.90H_2O + 3.92CO_2 + 4.02Pi$
$MR_5(NO_3)$		$4.64GAP + 2.04O_2 + 0.99NO_3 + 0.98H + 0.02SO_4 + 0.01Mg_2 \rightarrow B + 5.39CO_2 + 2.90H_2O + 4.51Pi$
$MR_6(NH_4)$	Biomass synthesis	$4.15\ SUC + 7.30H + 4.61O_2 + 0.99NH_4 + 0.12Pi + 0.02SO_4 + 0.01Mg_2 \rightarrow B + 7.04H_2O + 8.06CO_2$
$MR_6(NO_3)$		$4.90SUC5.28O_2 + 0.99NO_3 + 0.12Pi + 10.78H + 0.02SO_4 + 0.01Mg_2 \rightarrow B + 11.07CO_2 + 8.31H_2O$
$MR_7(NH_4)$	Biomass synthesis	$2.07\ GLC + 2.54O_2 + 0.99NH_4 + 0.12Pi + 0.02SO_4 + 0.01Mg_2 \rightarrow B + 3.91CO_2 + 7.04H_2O + 0.99H$
$MR_7(NO_3)$		$2.34GLC + 2.14O_2 + 0.99NO_3 + 0.12Pi + 0.98H + 0.02SO_4 + 0.01Mg_2 \rightarrow B + 5.49CO_2 + 7.63H_2O$

Table 2: List of the macroscopic reactions in each respective subnetwork. For biomass production, the stoichiometric values differ if the nitrogen source is nitrate or ammonium.

using minimal hypotheses, and when possible applying a mass action law. A list of all sub-networks and the macroscopic reactions can be found at Table 2.

2.3.2. Glyoxysome subnetwork

The glyoxysome pathway consists of 26 reactions, from which 8 are exchange reactions. The glyoxysome is the peroxysome compartment where the glyoxylate cycle occurs. Here carbon compounds are converted to succinate, also allowing the production of glucose from lipids. In this compartment, fatty acids can be used as a source of energy and carbon for growth is produced when no photosynthesis takes place. Two EFMs have been achieved for this subnetwork (MR1 and MR2). In the glyoxysome, butyrate and acetate are converted into acetyl-CoA, which is in turn converted, via the glyoxylate cycle, into succinate. The succinate then enters the cytosol and is injected into the Krebs cycle, thus producing the different metabolites necessary for the synthesis of biomass.

Butyrate is known for inhibiting algal growth under heterotrophic and mixotrophic conditions (Turon et al., 2015a). Furthermore, acetate inhibits the absorption of butyrate, thus leading to diauxic growth (Turon et al., 2015a). Thereby, Michaelis-Menten kinetics have been proposed to describe the absorption of acetate (α_{MR1}).

$$\alpha_{MR_1} = \frac{k_{MR1}.ACE}{KS_{MR1} + ACE} \tag{3}$$

For butyrate (α_{MR2}) Haldane kinetics have been chosen with an inhibition by acetate term.

$$\alpha_{MR2} = \frac{k_{MR2}.BUT}{BUT + \frac{k_{MR2}}{\beta_{MR2}}.(\frac{BUT}{Sopt_{MR2}} - 1)^2} \frac{k_d}{(ACE + k_d)} \tag{4}$$

2.3.3. Chloroplast subnetwork

The chloroplast subnetwork is composed of 21 reactions, from which 7 are exchange reactions. The glycerate-3-phosphate produced by photosynthesis is assumed to be transferred from the chloroplast towards the cytosol where it can be converted by glycolysis into glucose-6-phosphate or pyruvate. These metabolites are essential for the synthesis of functional biomass.

For autotrophic growth, light drives the reaction rate. When algae are growing on a turbid medium like wastewater, the average light intensity stays low and the local photoinhibition impact can be neglected (Martínez et al., 2018). Also under mixotrophic conditions with elevated concentration of carbon substrates, large biomass densities can be reached. Dense microalgal cultures strongly attenuate light. In line with Baroukh et al. (2017), photosynthesis rate is assumed to be linearly depending upon the average light intensity I_μ in the culture (see Equation 6).

Moreover, light attenuation in the culture medium is expected to follow the Beer-Lambert law. The light intensity at depth z depends on the incident light I_0 and the extinction coefficient α due to the biomass (the turbidity of the medium without algae is negligible):

$$I(z) = I_0.e^{-\alpha.z.B} \tag{5}$$

The average light intensity of the culture medium in the reactor of depth L is given as follows (with $\beta_{MR3} = \alpha.L$):

$$I_\mu = \frac{I_0}{L}\int_0^L e^{-\alpha.B.z}dz = \frac{I_0(1-e^{-\beta_{MR3}.B})}{\beta_{MR3}.B} \tag{6}$$

The kinetics in the chloroplast subnetwork is finally given by:

$$\alpha_{MR3} = \ k_{MR3}.I_\mu \tag{7}$$

2.3.4. Glycerol absorption subnetwork

The glycerol pathway subnetwork consists of 5 core reactions, plus the exchange reactions. Only one EFM was found for the glycerol absorption subnetwork (MR4).

The glycerol in the medium is transferred to the cytosol. Within three steps, it is transformed into glycerate-3-phosphate. During glycolysis, this glycerate-3-phosphate is then used for the synthesis of precursor metabolites that are in turn required for the synthesis of functional biomass. Since inhibition has been observed for glycerol assimilation (Chen and Walker, 2011, Ma et al., 2016, Liang et al., 2009), a Haldane reaction kinetics with inhibition was chosen (α_{MR4}):

$$\alpha_{MR4} = \ \frac{k_{MR4}.GLY}{GLY + \frac{k_{MR4}}{\beta_{MR4}}.(\frac{GLY}{Sopt_{MR4}} - 1)^2} \tag{8}$$

2.3.5. Functional biomass synthesis subnetwork

The reactions for the synthesis of lipids, proteins, DNA, RNA, chlorophyll and carbohydrates are all lumped together in the functional biomass synthesis subnetwork. This subnetwork includes glycolysis, the Krebs cycle, oxidative phosphorylation, the pentose phosphate pathway, carbohydrate, lipid, amino-acid and nucleotide synthesis, as well as the assimilation of nitrogen, sulphur and glucose. In total there are 141 reactions in the functional biomass subnetwork.

This subnetwork generated $86,167$ EFMs, including 3310 that did not produce biomass. Nearly all of the calculated EFMs are part of the biomass synthesis network. They can be sorted by using a similar method to the FBA (Flux Balance Analysis). The standard hypothesis supporting FBA is that evolution has selected metabolisms maximising biomass growth on each substrate (Orth et al., 2010), or

equivalently, minimising the loss of carbon as CO_2. Therefore, for each substrate, the EFM presenting the highest GAP/BIOM, SUC/BIOM and GLC/BIOM yields were selected. In this way, the use of GAP, SUC or GLC for the synthesis of biomass resulted from three macroscopic reactions (MR5, MR6 and MR7). The yield of biomass on the carbon substrate depends on the nitrogen source (NH_4 or NO_3). Table 1 shows the resulting macroscopic reactions for both cases.

Glycerate-3-phosphate originates from the chloroplast and from the assimilation of glycerol. It is injected into the glycolysis so as to produce the necessary metabolites for growth (α_{MR5}). The kinetics is supposed to be linear with respect to glycerate-3-phosphate (GAP):

$$\alpha_{ME5} = k_{MR5}.GAP \tag{9}$$

Succinate originates from the glyoxysome. It enters the Krebs cycle, thus also leading to the production of metabolites required for growth (α_{MR6}). Assuming a linear kinetics we get:

$$\alpha_{MR6} = k_{MR6}.SUC \tag{10}$$

Glucose in the medium is transferred to the cytosol where it enables the production of biomass. Glucose is inhibiting at high concentration (osmotic stress), and its consumption is assumed to follow a Haldane kinetics (α_{MR7}) (Azma et al., 2011, Wu and Shi, 2007, Liang et al., 2009). MR7:

$$\alpha_{MR7} = \frac{k_{MR7}.GLC}{GLC + \frac{k_{MR7}}{\beta_{MR7}}.(\frac{GLC}{Sopt_{MR7}} - 1)^2} \tag{11}$$

2.4. Global dynamics of the network

Finally, the dynamical evolution of the metabolic fluxes associated to the 188 considered metabolic core reactions can be derived from a system with 17 ordinary differential equations comprising 17 metabolites and 7 macroscopic reactions:

$$\frac{dM^{"}}{dt} = \frac{d\begin{pmatrix} S \\ A \\ B \end{pmatrix}}{dt} = K^{"}.\alpha.B - DM^{"} + DM^{"}_{in} \tag{12}$$

Where $M^{"}$ is the metabolite vector (17x1) comprising the substrates S, the metabolites that can accumulate A (SUC and GAP) and the functional biomass B. K' is the stoichiometric matrix (17x7) of the macroscopic reactions and α the associated kinetics vector (7x1). It is worth noting that, even if the model results from a reduction process through the DRUM approach, it can still predict the evolution of the 188 metabolic fluxes in the cell:

Moreover, the total biomass comprising the functional biomass and the metabolites A can be described as follows:

$$X_z(t) = \sum_A Z_A.A(t) + Z_B.B(t) \tag{13}$$

Where Z is a chemical element ($Z \in \{C; N; O; H; P; \ldots\}$), Z_A and Z_B are the number of chemical elements Z per mole of metabolites A and biomass B, $A(t)$ and $B(t)$ are the concentrations of A and B at time t $X_Z(t)$ is the concentration of the chemical element in the total biomass X at time t.

Finally, the metabolic fluxes within the whole network can be derived from the α kinetics and the elementary modes associated to the $E_{SN_i}, i \in 1, 2, 3$ subnetworks:

$$v = \begin{pmatrix} v_{SN_1} \\ \ldots \\ v_{SN_k} \end{pmatrix} = \begin{pmatrix} E_{SN_1} .\alpha_{SN_1} \\ \ldots \\ E_{SN_k}.\alpha_{SN_k} \end{pmatrix} \tag{14}$$

2.5. Sensitivity analysis

We calculate the sensitivity coefficient for the model parameters as defined in Bernard et al. (2001):

$$\sigma_y^{\Delta p} = \frac{1}{t_f} \int_0^{t_f} \frac{y(p + \Delta p, x_0, u, \tau) - y(p, x_0, u, \tau)}{y(p, x_0, u, \tau)} d\tau \tag{15}$$

where y is the simulated output at time τ with parameter set p, initial condition x_0 and input variables u (e.g. light intensity and dilution rate). We calculate the global sensitivity using Morris's sampling method implemented in the SALib Python toolbox (Morris, 1991, Herman and Usher, 2017), replacing the standard elementary effect by the sensitivity coefficient defined above. We analyse the region between $\pm 20\%$ of the calibrated values of the parameters. The analysis is conducted separately for each of the four carbon substrates in mixotrophic conditions at a light intensity of 500 $\mu mol/(m^2.s)$. $\sigma_y^{\Delta p}$ is calculated as the average of the simulations considering a cultivation of 6 hours and three different initial concentration of the considered carbon substrate (0.1, 1 and 10 g/L). Table 3 shows the result of the sensibility analysis for all the parameters.

2.6. Reduced model calibration

In order to calibrate, and then validate the model, a large set of experiments from the literature have been used. In total 122 selected experiments (see Table 1) gather data on growth i) under autotrophic conditions, without any organic carbon input and submitted to light intensities ranging from 30 to 540 $\mu E.m^{-2}.s^{-1}$ ii) under heterotrophic conditions, without any light, and with varying concentrations

Table 3: Kinetic parameters obtained after model calibration. Results of sensibility analysis ($\sigma_y^{\Delta p}$ and standard deviation (SD) of $\sigma_y^{\Delta p}$. Parameters calibrated in this work ^{A} and in Baroukh et al. (2017) ^{B}. MB: mole of biomass

Parameter	Value	Unit	$\sigma_y^{\Delta p}$	SD $\sigma_y^{\Delta p}$	Ref.
k_{MR1}	3.79 10^{-1}	$M.h^{-1}.MB^{-1}$	4.5910^{-03}	2.5210^{-03}	B
KS_{MR1}	5.50 10^{-5}	M	9.2010^{-05}	5.2410^{-03}	B
k_{MR2}	3.60 10^{-2}	$Mh^{-1}.MB^{-1}$	9.9610^{-05}	1.4010^{-03}	B
$Sopt_{MR2}$	1.90 10^{-5}	M	2.4810^{-04}	1.4110^{-03}	B
β_{MR2}	2.58 10^{5}	$h^{-1}.MB^{-1}$	1.8910^{-04}	1.4010^{-03}	B
k_{MR3}	1.90 10^{-3}	$Mh^{-1}.MB^{-1}.(m^2.s.\mu mol^{-1})$	9.2110^{-04}	5.7010^{-04}	B
β_{MR3}	2.48 10^{3}	MB^{-1}	-5.3810^{-04}	8.8210^{-05}	B
k_{MR4}	1.01	$M.h^{-1}.MB^{-1}$	5.5410^{-04}	1.8610^{-03}	A
$Sopt_{MR4}$	7.00 10^{-2}	M	9.2710^{-04}	2.2510^{-03}	A
β_{MR4}	9.05	$h^{-1}.MB^{-1}$	1.1010^{-04}	2.4310^{-03}	A
k_{MR5}	2.82 10^{1}	$h^{-1}.MB^{-1}$	9.7310^{-04}	1.1610^{-03}	B
k_D	5.39 10^{-10}	M	-1.1010^{-04}	1.4310^{-03}	B
k_{MR6}	2.37 10^{5}	$h^{-1}.MB^{-1}$	3.0710^{-06}	3.3310^{-03}	B
k_{MR7}	6.81 10^{-2}	$M.h^{-1}.MB^{-1}$	2.3910^{-03}	2.1610^{-03}	A
$Sopt_{MR7}$	5.07 10^{-2}	M	9.5410^{-05}	3.2210^{-03}	A
β_{MR7}	2.95 10^{+1}	$h^{-1}.MB^{-1}$	4.2410^{-04}	3.2410^{-03}	A

in acetate, butyrate, glucose and glycerol, pure or combined iii) under mixotrophic conditions, with light and varying concentrations in acetate, butyrate, glucose and glycerol. Depending on the studies, different combinations of these substrates were tested.

Only the parameters for glucose and glycerol consumption were calibrated. All the other kinetic parameters for the macro reactions are taken from Baroukh et al. (2017). The calibration was done following a two-step process. First a stochastic global optimizer, Differential Evolution algorithm (Storn and Price, 1997), calculates the set of parameters minimizing the relative error between model and experimental data of biomass and substrate concentration over time. This parameter set is, then, used as initial point in a Markov Chain Monte Carlo sampler, which returns the parameters set inside a confidence interval (Foreman-Mackey et al., 2013). Glucose kinetics parameters were calibrated using concentration data from 5 experiments of Li et al. (2013), while glycerol parameters were fitted using data from 6 experiments of Ma et al. (2016). Table 3 shows the value of calibrated parameters and Figure 2 shows the simulation of the calibrated model together with the experimental data used for calibration.

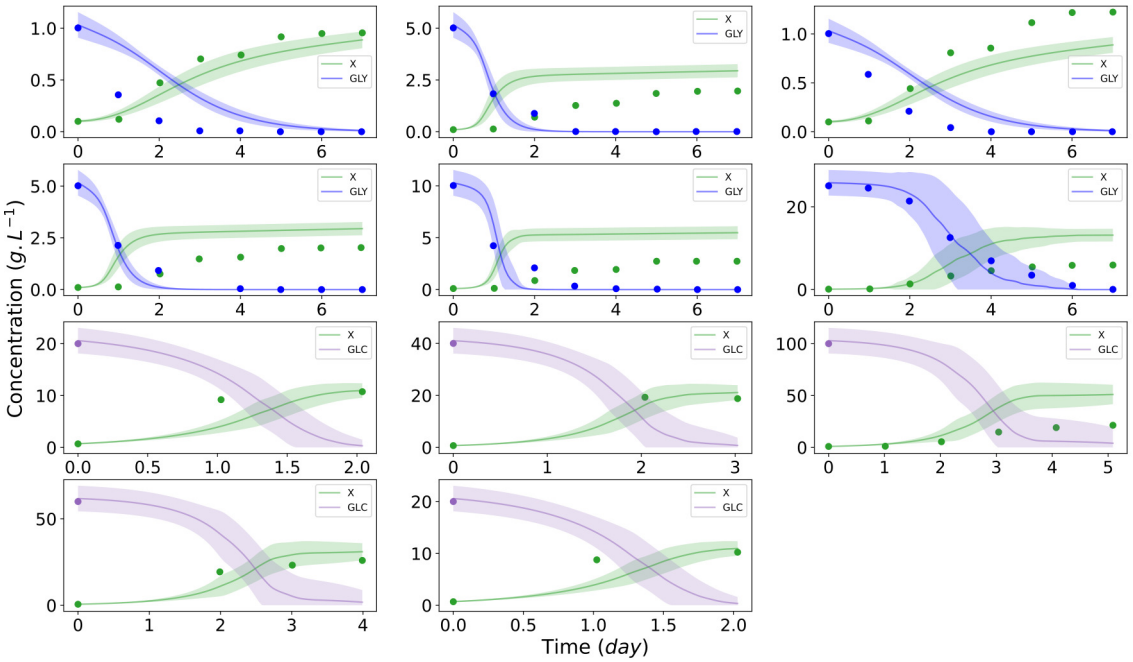

Figure 2: Comparison of the model against experimental data used for the calibration of glucose and glycerol kinetic parameters. Lines represent the average of 100 simulations and the colored region represents ± 1 standard deviation of estimated concentrations using Markov Chain Monte Carlo method.

2.7. Optimization of butyrate consumption

We consider the optimal control problem (Harmand et al., 2019), whose objective is to minimize the time t_f, where the chemical oxygen demand of the remaining waste substrates falls below the regulation threshold. The control variable is the concentration of the substrate to be added to the dark fermentation effluent (glucose or glycerol).

$$\min_{S_0} t_f : S(t_f) \leq \bar{S} \tag{16}$$

To solve the minimization problem we use a Nelder-Mead algorithm (Gao and Han, 2012). The output function simulates the metabolic model for a given S_0 returning t_f, the time required to reach the regulation threshold.

3. Results and discussion

3.1. Validation of the model

The experimental data not used during the calibration stage were used to validate the model. A coherent set of experiments, representing various experimental

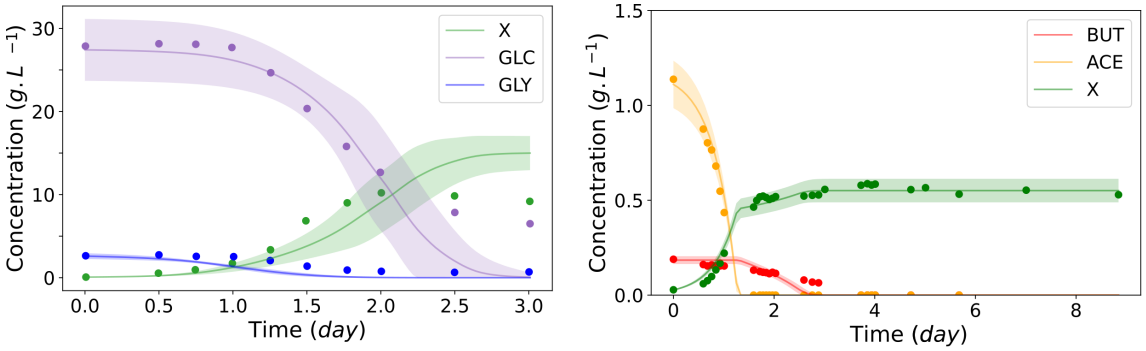

Figure 3: Model simulation and experimental data with two substrates. From left to right: glycerol and glucose; butyrate and acetate. The line represents the average of 100 simulations and the colored region represents ±1 standard deviation of estimated concentrations using Markov Chain Monte Carlo method.

conditions, was kept for this validation stage (see Table 1). We used a Markov Chain Monte Carlo method to select parameters (Foreman-Mackey et al., 2013). We considered a ±20% uncertainty in the initial concentration of substrates. In Figure 3, the results of the model simulations are compared with the experimental data with more than one substrate.

As illustrated in Figure 2 for single substrates, the model efficiently predicts the production of biomass and the consumption of substrates, whether in autotrophic, heterotrophic or in mixotrophic conditions. Furthermore, the model is still accurate when there are two substrates (Figure 3). More generally, the predictive performance of the model is summarized in the Taylor diagram in Figure 4 for the whole data set. This diagram represents at the same time the standard deviation of the biomass prediction error and the Pearson correlation coefficient (Taylor, 2001). It illustrates both the centered and reduced quadratic errors between the experimental data sets and the associated simulations, as well as the correlation between the model and the data. It thus summarizes the degree of resemblance between the data and the simulations for the vast range of considered data. Indeed, the closer a data point is to (0;1), the better the model reproduces the experimental data (Taylor, 2001). Figure 5 represents all the data points versus model prediction, also demonstrating the goodness of fit of the model.

The results of the sensibility analysis is also show in Table 3. Most parameters have the same order of sensibility (10^{-4}) showing that all have an importance in the model. The high standard deviation of the sensibility coefficient demonstrates the intertwined influence of parameters, for example maximum uptake rate and the optimal concentration of the substrate, also and the dependence of the actual substrate and biomass concentration in the dynamics of the system. This demonstrates the necessity of calibrating the model in a wide range of conditions.

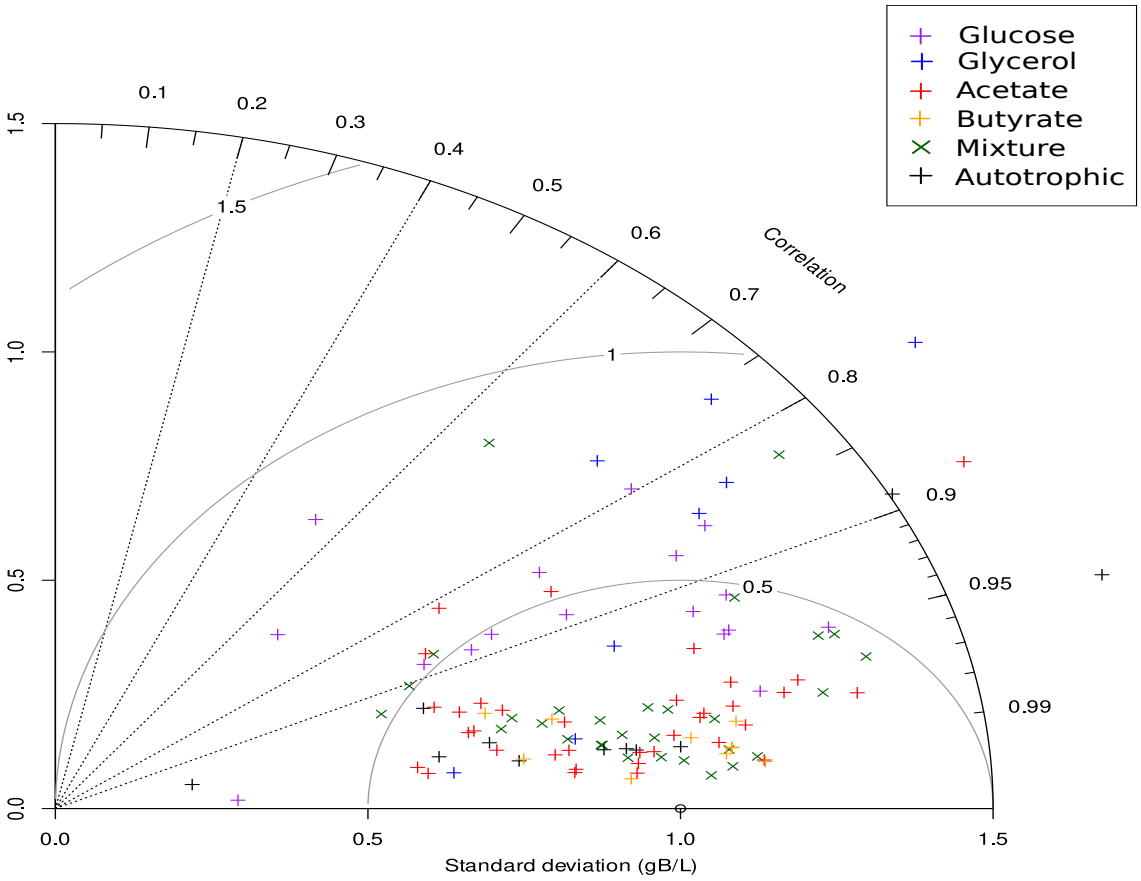

Figure 4: Taylor Diagram where each point represents the Pearson correlation coefficient and a normalized standard deviation of one experiment and model simulation. The semi circles centered at standard deviation 1.0 show the root-mean-square error.

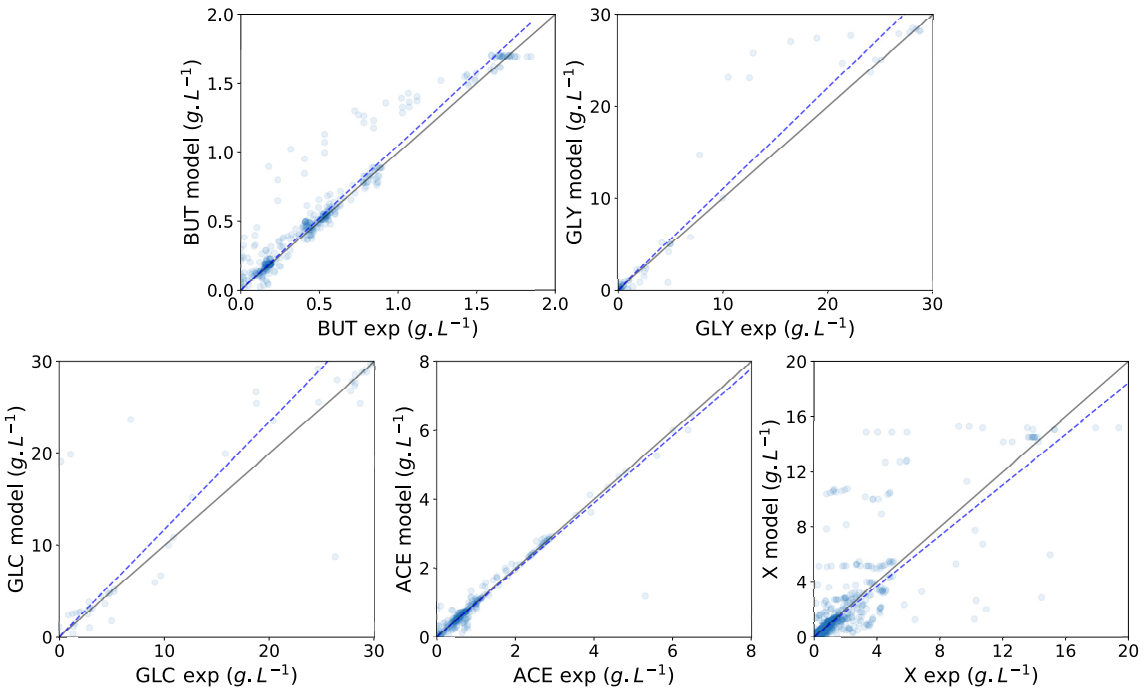

Figure 5: Validation of model predictions based on experimental data of butyrate, glycerol, glucose, acetate and biomass. All p-values for the regression are below 10^{-3}. R^2 for the lines are, respectively, 0.97, 0.71, 0.95, 0.97 and 0.64. Darker colors represent a concentration of data points.

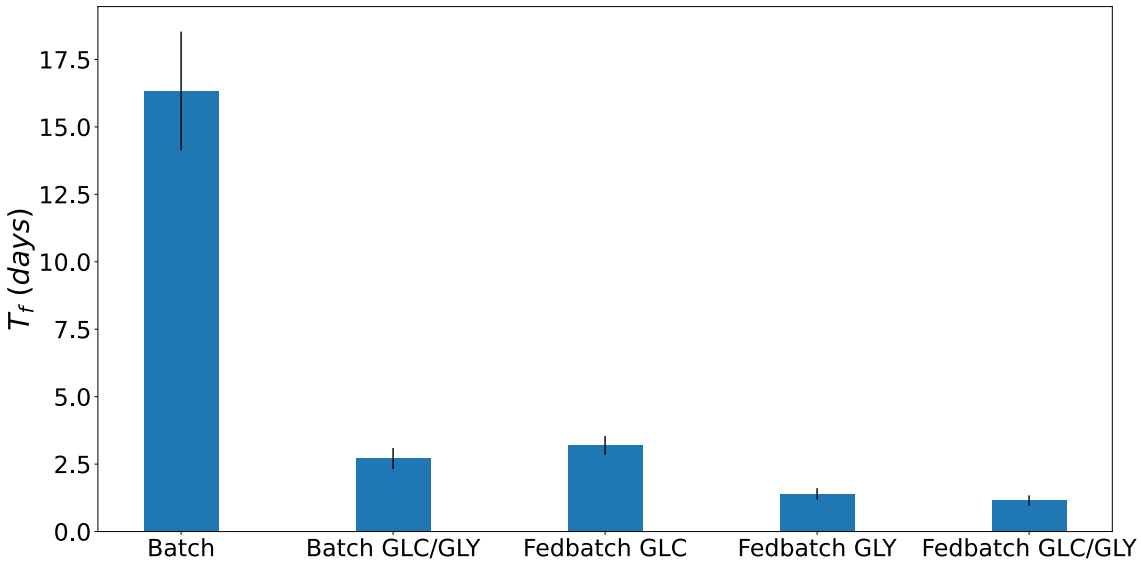

Figure 6: Time to reach the regulation threshold of a typical dark fermentation effluent using different conditions of cultivation - Batch (typical waste effluent), Batch GLC/GLY (typical waste with addition of an optimal concentration of glucose and glycerol), Fed-batch GLC, GLY, GLC/GLY (typical waste feeding, respectively, glucose, glycerol and a mixture of both.)

3.2. Optimization of microalgae growing on a mixture of dark fermentation products

Acetate and butyrate are the main volatile fatty acids (VFA) products of dark fermentation. Butyrate will inherently lead to growth inhibition, and a strategy must be found to unblock this inhibition. Here, we propose a strategy to enhance batch and fed-batch cultivation of microalgae from dark fermentation wastes, by adding glucose and glycerol. We first study mixotrophic conditions, considering a typical effluent from dark fermentation with $3.5g/L$ of butyrate and $1.7g/L$ of acetate (Lacroux et al., 2020, Ghimire et al., 2015) and a continuous light intensity of 500 $\mu mol/(m^2.s)$. The objective was that the chemical oxygen demand (COD) of the effluent at the end of the effluent treatment must be below $\bar{S}$ (here $\bar{S} = 125mg/L$) so that it can satisfy the state policies for discharge in the environment. We call this objective the regulation threshold. We solve the resulting optimal control problem in minimal time, with the objective that the COD of the remaining waste substrates falls below the regulation threshold. The control variable is the concentration of the substrate to be added to the dark fermentation effluent (glucose or glycerol). In the initial situation, without addition of organic carbon substrates, 16 days are necessary to reach the the regulation threshold.

Considering that glucose can be added, it turns out that the addition $98g/L$ of glucose reduces the time to reach the COD threshold to 4.0 days (see Figures 6 and 7). Using only glycerol takes longer: 5.6 days with an addition of $39.5g/L$ glycerol. Using a mixture of both substrates, the optimal starting concentration for the batch

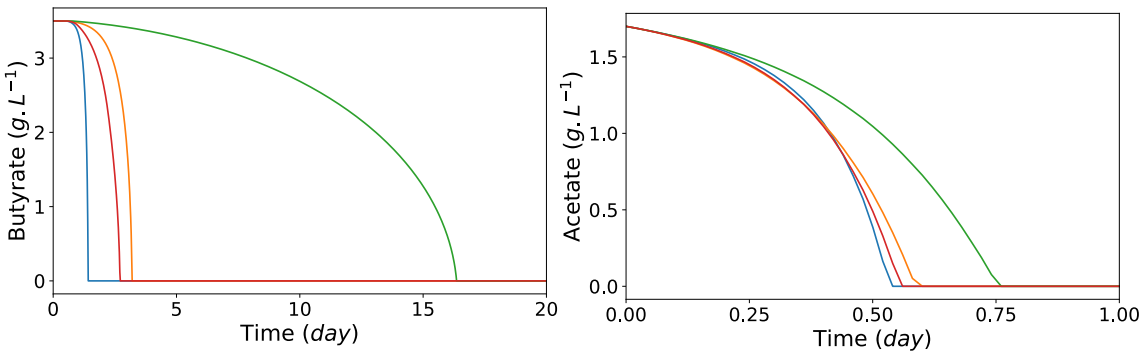

Figure 7: Concentrations of butyrate and acetate over time in different cultivation conditions. Optimal fed-batch with glycerol (blue), optimal fed-batch with glucose (red), batch with optimal addition of glycerol and glucose (orange), batch with only butyrate and acetate as substrates (green).

is $115g/L$ of glucose and $19g/L$ of glycerol, reducing the time to consume the VFAs to only 2.7 days.

Considering now a fed-batch cultivation systems instead of a batch one, the minimisation problem can be rewritten as following:

$$\min_{D} t_f : S(t_f) \leq \bar{S} \tag{17}$$

where D is the dilution rate of the inflow containing only the additional substrates, at a high concentration, so that the volume of the reactor does not change. t_f is the time to reach the regulation threshold. The optimal strategy can be approximated into a sub-optimal strategy, which would maximize the reaction rates for glucose and glycerol consumption. The strategy thus consists in computing the dilution rate such that glucose and glycerol concentrations stay constant close to the values for which the consumption of glucose and glycerol is maximum. The control problem is then reduced to finding the optimal final time of the inlet flux in the cases of a glucose, glycerol, and mixture inlet. In the case of the mixture, a fraction of 0.21 of glucose and 0.79 of glycerol is obtained, keeping glycerol at an optimal concentration. Using this control strategy, the final times for fed-batch cultivation are: 3.2 days for glucose, 1.4 days for glycerol and 1.2 days for a mixture of glucose and glycerol (see Figure 6), to be compared to the 16 days whithout inorganic carbon addition.

3.3. Analysis of metabolic maps

One of the advantages of metabolic model is that the main metabolic fluxes can be estimated. They are represented in Figure 8 considering the exponential growth phase. During autotrophic growth, a strong activity takes place in the chloroplast subnetwork where photosynthesis occurs. The greatest fluxes are associated to the fixation of CO_2 by RUBISCO, the conversion to 3PG (3-phosphoglycerate) and the

conversion of 3PG to glycerate-3-phosphate (GAP). GAP is then mainly transported toward the cytoplasm, where it is injected into the glycolysis. From then on, it enables the synthesis of precursor metabolites that are necessary for the synthesis of functional biomass composed of proteins, DNA, RNA, chlorophyll, carbohydrates, and lipids. During pure heterotrophic growth, in the dark, no reaction occurs in the chloroplast subnetwork. Considering a a mix of acetate or butyrate, the largest fluxes are concentrated in the glyoxysome subnetwork where carbon substrates are converted into succinate. The synthesised succinate is exported from the glyoxysome and injected into the Krebs cycle. The latter then enables the synthesis of precursor metabolites for the production of functional biomass. To ascend the glycolysis, the anaplerotic pathways are in an upward direction.

No reaction takes place in the glyoxysome, neither in the glycerol utilization pathway for growth on glucose only. Glucose carried from the medium into the cytoplasm is directly injected into the upper glycolysis for the production of precursor metabolites necessary for the synthesis of functional biomass. Glycolysis is therefore entirely in a downward direction, as the anaplerotic pathways that enable the synthesis of oxaloacetate (OXA) fueling the Krebs cycle.

For growth on glycerol only, the greatest fluxes are located in the glycerol utilization pathway subnetwork, where the uptaken glycerol is converted to glycerate-3-phosphate. The glycerate-3-phosphate is then injected into the middle of glycolysis, this time in an upward direction for the high glycolysis and in a downward direction for the lower glycolysis. The remnants of the fluxes are similar to those observed for glucose.

In mixotrophic conditions, when all carbon substrates are present in the medium, all metabolic reactions are activated. First, diauxic growth occurs, and acetate is consumed instead of butyrate. Glycerol and glucose are also used, but the flux remains after the acetate is depleted. Secondly, once all acetate has disappeared, butyrate is in turn consumed.

Figure 8 shows the metabolic fluxes after 30 hours of batch culture with optimal initial conditions (110 g/l of glucose and 20 g/L of glycerol). At this point, the acetate in the culture is practically depleted, but the concentration of butyrate remains similar to the initial condition. The rate of consumption of butyrate then remains stable for 2 days, and the rate rapidly increases until the concentration threshold is reached. Since the optimal concentration is about 40 times lower than the regulation threshold, the butyrate consumption rate does not reach the maximum value. Glycerol has a much lower concentration, while the flux of glucose concentration is still high. As a result of the higher concentration of biomass and the lower availability of light per cell, the metabolic fluxes in the chloroplast are reduced.

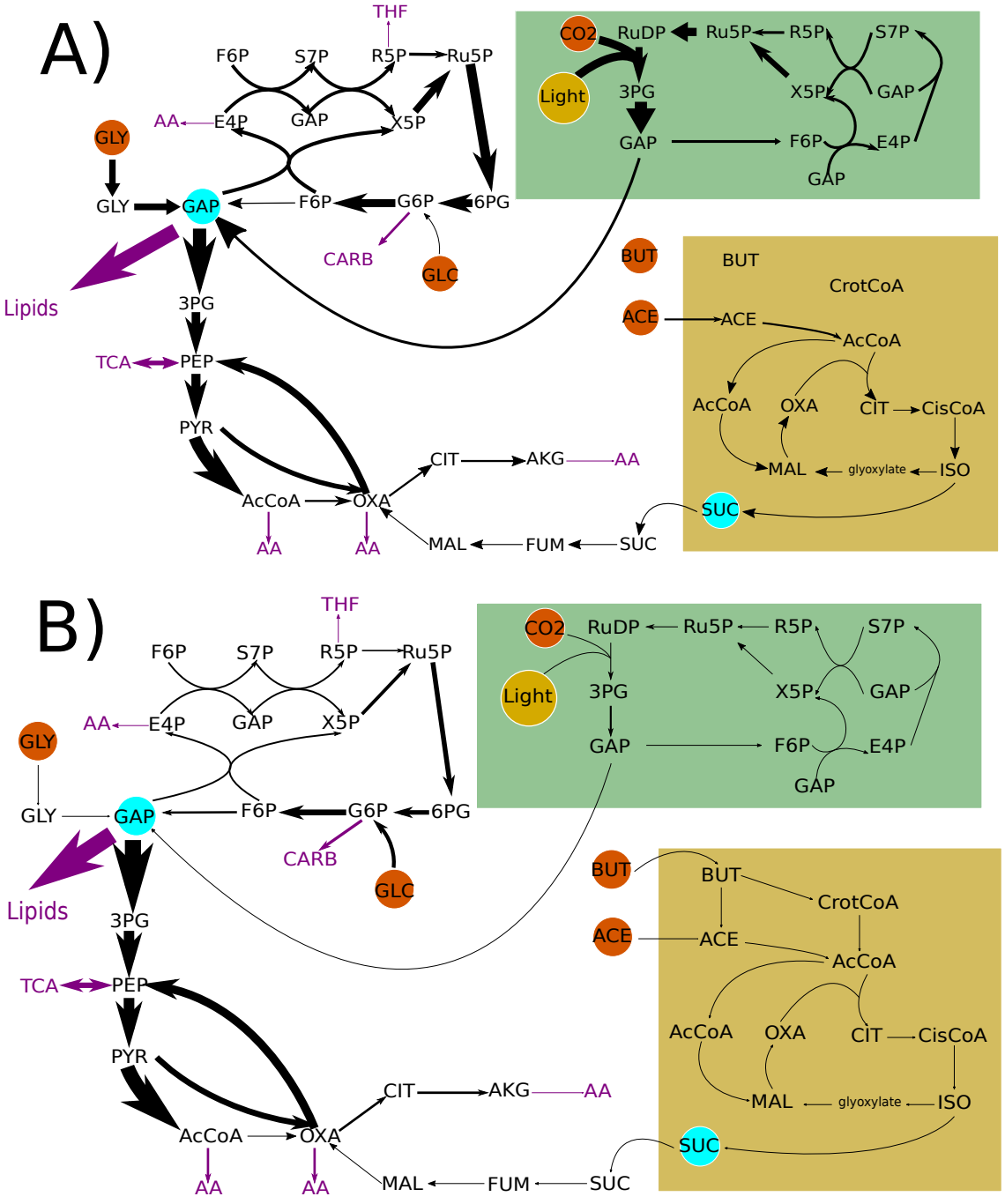

Figure 8: Metabolic charts showing the fluxes of an optimized batch. Above, A, at initial concentration of acetate and butyrate with optimal conditions of glucose and glycerol. Below, B, 30 hours after the beginning of the batch. The widths are linearly proportional to the calculated flux.

3.4. Model limitations and perspectives

The reduced metabolic model efficiently represents the microalgal growth under various substrates in heterotrophic or mixotrophic conditions. More accurate predictions could probably be obtained by expanding the model to include other factors such as pH, CO_2, O_2 and temperature which were differing among the large experimental data set considered in our study. According to Lacroux et al. (2020), pH fluctuations when algae consume VFA can strongly impact growth and should now be included in the model. Associating a pH model that accounts for the various chemical species and their speciation, as proposed by Casagli et al. (2021a), would allow the calculation of the pH and the concentration of the undissociated form of the acids, which is the one actually taken up by the microalgae.

The effect of mixotrophic growth, here considered as the sum of autotrophic and heterotrophic conditions, can be more subtle in some cases. There is no consensus in the literature for a general model that fits all cases. For example, according to Martínez and Orús (1991), mixotrophic growth is greater than the sum of autotrophic and heterotrophic conditions when the concentration of CO_2 is limiting, since CO_2 produced by respiration can be recycled for the photosynthesis pathway. Recently, circular use of CO_2 and O_2 and preferential consumption of inorganic carbon has also been evidenced for *Chlorella vulgaris*, nonetheless heterotrophic growth was promoted at high 0_2 concentrations (Manhaeghe et al., 2020). Furthermore, under certain conditions an inverse relationship between light intensity and glucose consumption has been recorded (Patel et al., 2019, Wan et al., 2011).

Temperature is one of the most important factors affecting microalgae growth, even if only a minority of the models account for it (Shoener et al., 2019). The experimental data considered here were carried out at various temperatures and accounting for it would increase model accuracy. In the case of metabolic models, including temperature is challenging, and will involve a large number of parameters to characterize the influence of temperature on each individual reaction. The influence of short variations of temperature could be well estimated by the Arrhenius equation, but large variations of temperature typically occurring in outdoor cultivation require more advanced models (Casagli and Bernard, 2022, Pessi et al., 2022). For these reasons, calibrating the temperature effect would require a large amount of dedicated experiments.

It is likely that other factors were influencing the experimental outcomes in the considered data base, especially for the experiments carried out with high concentrations of glucose and glycerol. It seems that another substrate was sometimes limiting growth, most probably nitrogen according to the mass balance from the medium initial composition.

Extending the metabolic model to account for all these mechanisms is beyond the scope of this paper. It will require a large number of experiments to further

calibrate and validate the model. Our objective was primarily to validate the model across a wide range of conditions, demonstrating a strong foundation for future improvements in the model, knowing that most models of water resource recovery facilities are calibrated, but not validated (Shoener et al., 2019). Overall, despite the simplicity of the model in its present form, it is already very efficient. Especially when accounting for the diversity of strain and experimental conditions considered through the 15 studied papers. The model can then, already in its present form, can be used as a tool for optimizing microalgae growth on a mix of substrates.

Better predictions will be achieved if biochemical and also cellular level processes (e.g. metabolic reactions) are considered in the next generation of water treatment models (Batstone et al., 2019). Metabolic models are able to accurately predict the specific VFAs produced by a mixed-culture depending on the components of the input medium (Regueira et al., 2020). We could envisage the coupling of these models - VFA production by mixed-culture and treatment by microalgae - to optimize production of hydrogen constrained by the capacities of the waste treatment system, or to predict in advance the necessity of adding another carbon substrate such as glycerol. Metabolic knowledge could also give a strong foundation for estimating possible medium conditions take could lead to undesirable emissions, such as N_2O, and which are not well modeled through the current approaches (Casagli et al., 2021a).

4. Conclusion

The metabolic model developed in this work for *Chlorella* accurately predicts growth under autotrophic, heterotrophic and mixotrophic conditions with acetate, butyrate, glucose and glycerol for more than a hundred experiments from the literature. Covering a large range of conditions, strains and substrates, the predictive capacity of this reduced metabolic model remains remarkable. Moreover, to lift the inhibition exerted by the presence of butyrate, the optimal addition of different substrates in the medium has been predicted by the model. Optimising the cultivation conditions reduce the time to reach the regulation threshold from 16 to less than 2 days.

Thanks to this approach, it will become possible to streamline two-stage water treatment strategies, and to recycle, carbon, nitrogen and phosphorus into the microalgal biomass. In particular, this approach highlights noteworthy synergies between waste molecules, and the important role of of the metabolic network for future models. The anticipated management of these molecules could improve productivity significantly.

Acknowledgment

The authors acknowledge the support of the ControlAB ANR project (ANR-20-CE45-0014) and of the BIOMSA Ademe project. The UCAJEDI and EUR DS4H investments in the Future projects managed by the National Research Agency (ANR) with the reference numbers ANR-15-IDEX-0001.

References

Arashiro, L.T., Josa, I., Ferrer, I., Van Hulle, S.W.H., Rousseau, D.P.L., Garfí, M., 2022. Life cycle assessment of microalgae systems for wastewater treatment and bioproducts recovery: Natural pigments, biofertilizer and biogas. Sci. Total Environ. 847, 157615. doi:10.1016/j.scitotenv.2022.157615.

Azma, M., Mohamed, M.S., Mohamad, R., Rahim, R.A., Ariff, A.B., 2011. Improvement of medium composition for heterotrophic cultivation of green microalgae, Tetraselmis suecica, using response surface methodology. Biochem. Eng. J. 53, 187–195. doi:10.1016/j.bej.2010.10.010.

Baroukh, C., Muñoz-Tamayo, R., Bernard, O., Steyer, J.P., 2016. Reply to the Comment on "Mathematical modeling of unicellular microalgae and cyanobacteria metabolism for biofuel production" by Baroukh et al. [Curr. Opin. Biotechnol. 2015, 33:198–205]. Curr. Opin. Biotechnol. 38, 200–202. doi:10.1016/j.copbio.2016.02.018.

Baroukh, C., Muñoz-Tamayo, R., Steyer, J.P., Bernard, O., 2014. DRUM: A new framework for metabolic modeling under non-balanced growth. Application to the carbon metabolism of unicellular microalgae. PLOS ONE 9, 1–15. doi:10.1371/journal.pone.0104499.

Baroukh, C., Turon, V., Bernard, O., 2017. Dynamic metabolic modeling of heterotrophic and mixotrophic microalgal growth on fermentative wastes. PLoS Comput. Biol. 13, 1–18. doi:10.1371/journal.pcbi.1005590.

Barsanti, L., Gualtieri, P., 2018. Is exploitation of microalgae economically and energetically sustainable? Algal Res. 31, 107–115. doi:10.1016/j.algal.2018.02.001.

Batstone, D., Hülsen, T., Oehmen, A., 2019. Metabolic modelling of mixed culture anaerobic microbial processes. Curr. Opin. Biotechnol. 57, 137–144. doi:10.1016/j.copbio.2019.03.014.

Bernard, O., Hadj-Sadok, Z., Dochain, D., Genovesi, A., Steyer, J.P., 2001. Dynamical model development and parameter identification for an anaerobic wastewater treatment process. Biotechnol. Bioeng. 75, 424–438. doi:10.1002/bit.10036.

Casagli, F., Bernard, O., 2022. Simulating biotechnological processes affected by meteorology: Application to algae–bacteria systems. J. Cleaner Prod. 377, 134190. doi:10.1016/j.jclepro.2022.134190.

Casagli, F., Rossi, S., Steyer, J.P., Bernard, O., Ficara, E., 2021a. Balancing Microalgae and Nitrifiers for Wastewater Treatment: Can Inorganic Carbon Limitation Cause an Environmental Threat? Environ Sci Technol 55, 3940–3955. doi:10.1021/acs.est.0c05264.

Casagli, F., Zuccaro, G., Bernard, O., Steyer, J.P., Ficara, E., 2021b. ALBA: A comprehensive growth model to optimize algae-bacteria wastewater treatment in raceway ponds. Water Res. 190, 116734. doi:10.1016/J.WATRES.2020.116734.

Chen, C.Y., Ho, S.H., Liu, C.C., Chang, J.S., 2017a. Enhancing lutein production with Chlorella sorokiniana Mb-1 by optimizing acetate and nitrate concentrations under mixotrophic growth. J. Taiwan Inst. Chem. Eng. 79, 88–96. doi:10.1016/j.jtice.2017.04.020.

Chen, J.H., Chen, C.Y., Chang, J.S., 2017b. Lutein production with wild-type and mutant strains of Chlorella sorokiniana MB-1 under mixotrophic growth. J. Taiwan Inst. Chem. Eng. 79, 66–73. doi:10.1016/j.jtice.2017.04.022.

Chen, Y.H., Walker, T.H., 2011. Biomass and lipid production of heterotrophic microalgae Chlorella protothecoides by using biodiesel-derived crude glycerol. Biotechnol. Lett. 2011 3310 33, 1973–1983. doi:10.1007/S10529-011-0672-Y.

Espinosa-Gonzalez, I., Parashar, A., Bressler, D.C., 2014. Heterotrophic growth and lipid accumulation of Chlorella protothecoides in whey permeate, a dairy by-product stream, for biofuel production. Bioresour. Technol. 155, 170–176. doi:10.1016/J.BIORTECH.2013.12.028.

Foreman-Mackey, D., Hogg, D.W., Lang, D., Goodman, J., 2013. Emcee : The MCMC Hammer. Publ. Astron. Soc. Pac. 125, 306–312. doi:10.1086/670067.

Gao, F., Han, L., 2012. Implementing the Nelder-Mead simplex algorithm with adaptive parameters. Comput Optim Appl 51, 259–277. doi:10.1007/s10589-010-9329-3.

Gao, Y., Guo, L., Jin, C., Zhao, Y., Gao, M., She, Z., Wang, G., 2022. Metagenomics and network analysis elucidating the coordination between fermentative bacteria and microalgae in a novel bacterial-algal coupling reactor (BACR) for mariculture wastewater treatment. Water Res. 215, 118256. doi:10.1016/j.watres.2022.118256.

Ghimire, A., Frunzo, L., Pirozzi, F., Trably, E., Escudie, R., Lens, P.N., Esposito, G., 2015. A review on dark fermentative biohydrogen production from organic biomass: Process parameters and use of by-products. Appl. Energy 144, 73–95. doi:10.1016/j.apenergy.2015.01.045.

Hameri, T., Fengos, G., Hatzimanikatis, V., 2021. The effects of model complexity and size on metabolic flux distribution and control: Case study in Escherichia coli. BMC Bioinf. 22, 1–25. doi:10.1186/s12859-021-04066-y.

Harmand, J., Lobry, C., Rapaport, A., Sari, T., 2019. Optimal Control in Bioprocesses: Pontryagin's Maximum Principle in Practice. volume 3 of *Chemical Engineering Series - Chemostat and Bioprocesses*. Wiley.

Herman, J., Usher, W., 2017. SALib: An open-source Python library for Sensitivity Analysis. J Open Source Softw 2. doi:10.21105/joss.00097.

Hu, B., Min, M., Zhou, W., Du, Z., Mohr, M., Chen, P., Zhu, J., Cheng, Y., Liu, Y., Ruan, R., 2012. Enhanced mixotrophic growth of microalga Chlorella sp. on pretreated swine manure for simultaneous biofuel feedstock production and nutrient removal. Bioresour. Technol. 126, 71–79. doi:10.1016/j.biortech.2012.09.031.

Klamt, S., Stelling, J., 2003. Two approaches for metabolic pathway analysis? Trends Biotechnol. 21, 64–69. doi:10.1016/S0167-7799(02)00034-3.

Küken, A., Wendering, P., Langary, D., Nikoloski, Z., 2021. A structural property for reduction of biochemical networks. Sci Rep 11, 17415. doi:10.1038/s41598-021-96835-1.

Lacroux, J., Jouannais, P., Atteia, A., Bonnafous, A., Trably, E., Steyer, J.P., van Lis, R., 2022. Microalgae screening for heterotrophic and mixotrophic growth on butyrate. Algal Res 67, 102843. doi:10.1016/j.algal.2022.102843.

Lacroux, J., Trably, E., Bernet, N., Steyer, J.P., van Lis, R., 2020. Mixotrophic growth of microalgae on volatile fatty acids is determined by their undissociated form. Algal Res. 47, 101870. doi:10.1016/j.algal.2020.101870.

León-Vaz, A., Léon, R., Díaz-Santos, E., Vigara, J., Raposo, S., 2019. Using agro-industrial wastes for mixotrophic growth and lipids production by the green microalga Chlorella sorokiniana. N. Biotechnol. 51, 31–38. doi:10.1016/j.nbt.2019.02.001.

Li, T., Zheng, Y., Yu, L., Chen, S., 2013. High productivity cultivation of a heat-resistant microalga Chlorella sorokiniana for biofuel production. Bioresour. Technol. 131, 60–67. doi:10.1016/j.biortech.2012.11.121.

Li, T., Zheng, Y., Yu, L., Chen, S., 2014. Mixotrophic cultivation of a Chlorella sorokiniana strain for enhanced biomass and lipid production. Biomass Bioenergy 66, 204–213. doi:10.1016/j.biombioe.2014.04.010.

Liang, Y., Sarkany, N., Cui, Y., 2009. Biomass and lipid productivities of Chlorella vulgaris under autotrophic, heterotrophic and mixotrophic growth conditions. Biotechnol. Lett. 2009 317 31, 1043–1049. doi:10.1007/S10529-009-9975-7.

Ma, X., Zheng, H., Addy, M., Anderson, E., Liu, Y., Chen, P., Ruan, R., 2016. Cultivation of Chlorella vulgaris in wastewater with waste glycerol: Strategies for improving nutrients removal and enhancing lipid production. Bioresour. Technol. 207, 252–261. doi:10.1016/j.biortech.2016.02.013.

Manhaeghe, D., Blomme, T., Van Hulle, S.W., Rousseau, D.P., 2020. Experimental assessment and mathematical modelling of the growth of Chlorella vulgaris under photoautotrophic, heterotrophic and mixotrophic conditions. Water Res. 184, 116152. doi:10.1016/J.WATRES.2020.116152.

Martínez, C., Mairet, F., Bernard, O., 2018. Theory of turbid microalgae cultures. J. Theor. Biol. 456, 190–200. doi:10.1016/j.jtbi.2018.07.016.

Martínez, F., Orús, M.I., 1991. Interactions between Glucose and Inorganic Carbon Metabolism in Chlorella vulgaris Strain UAM 101. Plant Physiol. 95, 1150–1155. doi:10.1104/PP.95.4.1150.

Morales, M., Collet, P., Lardon, L., Hélias, A., Steyer, J.P., Bernard, O., 2019. Chapter 20 - Life-cycle assessment of microalgal-based biofuel, in: Pandey, A., Chang, J.S., Soccol, C.R., Lee, D.J., Chisti, Y. (Eds.), Biofuels from Algae (Second Edition). Elsevier. Biomass, Biofuels, Biochemicals, pp. 507–550. doi:10.1016/B978-0-444-64192-2.00020-2.

Morris, M.D., 1991. Factorial Sampling Plans for Preliminary Computational Experiments. Technometrics 33, 161–174. doi:10.2307/1269043.

Ogbonna, J.C., Masui, H., Tanaka, H., 1997. Sequential heterotrophic/autotrophic cultivation–an efficient method of producing Chlorella biomass for health food and animal feed. J. Appl. Phycol. 9, 359–366. doi:10.1023/A:1007981930676.

O'Grady, J., Morgan, J.A., 2011. Heterotrophic growth and lipid production of Chlorella protothecoides on glycerol. Bioprocess Biosyst. Eng. 34, 121–125. doi:10.1007/s00449-010-0474-y.

Orth, J.D., Thiele, I., Palsson, B.Ø., 2010. What is flux balance analysis? Nat. Biotechnol. 28, 245–248. doi:10.1038/nbt.1614.

Patel, A.K., Joun, J.M., Hong, M.E., Sim, S.J., 2019. Effect of light conditions on mixotrophic cultivation of green microalgae. Bioresour. Technol. 282, 245–253. doi:10.1016/J.BIORTECH.2019.03.024.

Pessi, B.A., Pruvost, E., Talec, A., Sciandra, A., Bernard, O., 2022. Does temperature shift justify microalgae production under greenhouse? Algal Res. 61, 102579. doi:10.1016/j.algal.2021.102579.

Rafrafi, Y., Trably, E., Hamelin, J., Latrille, E., Meynial-Salles, I., Benomar, S., Giudici-Orticoni, M.T., Steyer, J.P., 2013. Sub-dominant bacteria as keystone species in microbial communities producing bio-hydrogen. Int. J. Hydrogen Energy 38, 4975–4985. doi:10.1016/j.ijhydene.2013.02.008.

Regueira, A., Bevilacqua, R., Lema, J.M., Carballa, M., Mauricio-Iglesias, M., 2020. A metabolic model for targeted volatile fatty acids production by cofermentation of carbohydrates and proteins. Bioresour. Technol. 298, 122535. doi:10.1016/j.biortech.2019.122535.

Sajjadi, B., Chen, W.Y., Raman, A.A.A., Ibrahim, S., 2018. Microalgae lipid and biomass for biofuel production: A comprehensive review on lipid enhancement strategies and their effects on fatty acid composition. Renewable Sustainable Energy Rev. 97, 200–232. doi:10.1016/j.rser.2018.07.050.

Schuster, S., Dandekar, T., Fell, D.A., 1999. Detection of elementary flux modes in biochemical networks: A promising tool for pathway analysis and metabolic engineering. Trends Biotechnol. 17, 53–60. doi:10.1016/S0167-7799(98)01290-6.

Sen, R., Martin, G.J.O., 2018. Glycerol and nitrate utilisation by marine microalgae Nannochloropsis salina and Chlorella sp. and associated bacteria during mixotrophic and heterotrophic growth. Algal Res. 33, 298–309. doi:10.1016/j.algal.2018.06.002.

Shoener, B.D., Schramm, S.M., Béline, F., Bernard, O., Martínez, C., Plósz, B.G., Snowling, S., Steyer, J.P., Valverde-Pérez, B., Wágner, D., Guest, J.S., 2019. Microalgae and cyanobacteria modeling in water resource recovery facilities: A critical review. Water Res. X 2, 100024. doi:10.1016/j.wroa.2018.100024.

Singh, D., Lercher, M.J., 2020. Network reduction methods for genome-scale metabolic models. Cell. Mol. Life Sci. 77, 481–488. doi:10.1007/s00018-019-03383-z.

Storn, R., Price, K., 1997. Differential evolution–a simple and efficient heuristic for global optimization over continuous spaces. J. Global Optim. 11, 341–359. doi:10.1023/A:1008202821328.

Tan, X.B., Lam, M.K., Uemura, Y., Lim, J.W., Wong, C.Y., Lee, K.T., 2018. Cultivation of microalgae for biodiesel production: A review on upstream and downstream processing. Chinese J. Chem. Eng. 26, 17–30. doi:10.1016/j.cjche.2017.08.010.

Taylor, K.E., 2001. Summarizing multiple aspects of model performance in a single diagram. J. Geophys. Res. Atmos. 106, 7183–7192. doi:10.1029/2000JD900719.

Terzer, M., Stelling, J., 2008. Large-scale computation of elementary flux modes with bit pattern trees. Bioinformatics 24, 2229–2235. doi:10.1093/bioinformatics/btn401.

Turon, V., Baroukh, C., Trably, E., Latrille, E., Fouilland, E., Steyer, J.P., 2015a. Use of fermentative metabolites for heterotrophic microalgae growth: Yields and kinetics. Bioresour. Technol. 175, 342–349. doi:10.1016/j.biortech.2014.10.114.

Turon, V., Trably, E., Fouilland, E., Steyer, J.P., 2015b. Growth of Chlorella sorokiniana on a mixture of volatile fatty acids: The effects of light and temperature. Bioresour. Technol. 198, 852–860. doi:10.1016/j.biortech.2015.10.001.

Wágner, D.S., Valverde-Pérez, B., Sæbø, M., Bregua de la Sotilla, M., Van Wagenen, J., Smets, B.F., Plósz, B.G., 2016. Towards a consensus-based biokinetic model for green microalgae – The ASM-A. Water Res. 103, 485–499. doi:10.1016/j.watres.2016.07.026.

Wan, M., Liu, P., Xia, J., Rosenberg, J.N., Oyler, G.A., Betenbaugh, M.J., Nie, Z., Qiu, G., 2011. The effect of mixotrophy on microalgal growth, lipid content, and expression levels of three pathway genes in Chlorella sorokiniana. Appl. Microbiol. Biotechnol. 91, 835–844. doi:10.1007/s00253-011-3399-8.

Wu, Z., Shi, X., 2007. Optimization for high-density cultivation of heterotrophic Chlorella based on a hybrid neural network model. Lett. Appl. Microbiol. 44, 13–18. doi:10.1111/j.1472-765X.2006.02038.x.

Xie, Y., Li, J., Ho, S.H., Ma, R., Shi, X., Liu, L., Chen, J., 2020a. Pilot-scale cultivation of Chlorella sorokiniana FZU60 with a mixotrophy/photoautotrophy two-stage strategy for efficient lutein production. Bioresour. Technol. 314, 123767. doi:10.1016/j.biortech.2020.123767.

Xie, Z., Lin, W., Liu, J., Luo, J., 2020b. Mixotrophic cultivation of Chlorella for biomass production by using pH-stat culture medium: Glucose-Acetate-Phosphorus (GAP). Bioresour. Technol. 313, 123506. doi:10.1016/j.biortech.2020.123506.